STRESS ANALYSIS OF A 46-INCH REACTOR FEED/EFFLUENT EXCHANGER

Chris Alexander
Stress Engineering Services, Inc.
Houston, Texas

John Jagodzinski
Brown Fintube
Houston, Texas

Richard Biel, P.E.
Stress Engineering Services, Inc.
Houston, Texas

ABSTRACT

Stress Engineering Services, Inc. performed a series of analyses for Brown Fintube to determine the mechanical behavior of its high performance 46-inch reactor feed/effluent exchanger. Initial efforts focused on the global behavior of the exchanger subjected to pressure and thermal loads, while the ultimate objective addressed potential leakage in the main body flange. Using finite element analyses incorporating shell, solid, and continuum models, Stress Engineering was able to demonstrate that the sealing load of the flanges could be maintained even with elevated bolt temperatures up to 400°F. Using the methods permitted by the ASME Boiler & Pressure Vessel Code, Section VIII, Division 2, linearized stresses were calculated. All calculated stress intensities were less than the Division 2 allowable stresses. Based upon the results of the analyses, the design of the main body flange also met the stress design criteria per Division 1 of the Code. This project was a clear demonstration on how analysis methods can be used to solve complex engineering problems that include a wide range of variables and operating conditions. The conservative calculation techniques of Division 1 of the Code were also confirmed in this work.

INTRODUCTION

Brown Fintube (BFT) requested that Stress Engineering Services, Inc. perform a series of analyses to address the performance of an effluent exchanger subjected to large temperature differentials on the shellside inlet and outlet. Initial concerns were raised regarding the bowing of the tube bundle and shell in association with higher temperatures in the top region of the exchanger and their impact on potential leaking of the gaskets. The analytical efforts involved developing an understanding of the overall behavior of the exchanger. This included studies on the tube bundle, shell, supports, flange region, and tubesheet that included heat transfer and structural models. The analysis efforts determined stresses and deflections in the heat exchanger components. In additional to understanding the overall behavior, the analysis also addressed contact stresses developed in the gasket region of the main body flange. This latter concern was the primary point of interest as it related to sealing of the main body flange.

The primary analyses involved a combination of linear elastic half-symmetry finite element models using both four-node shell elements as well as eight-node brick elements. The former were used to address overall global behavior, while the latter involved contact elements to address variations in gasket sealing pressures associated with elevated temperatures and pressures. An axisymmetric model of the main body flange was also used to determine the effects of make-up stress due to bolting on the design.

MODELING TECHNIQUES

Analyses of the 46-inch reactor feed/effluent exchanger using finite element modeling were performed. This method of analysis permits evaluation of structures that involve complex geometries, loads, and boundary conditions. The heat exchanger considered in this study is complex in all three areas. The PATRAN modeling package was used for generating the finite element mesh of each of the models, while the ABAQUS (version 5.8) general-purpose finite element code was used for processing and post-processing the results. BFT provided the temperature and heat transfer conditions prior to starting the analysis.

Three types of finite element analysis (FEA) models were used in the study of the Brown Fin Tube heat exchanger. The first type of FEA model used a combination of quadrilateral shell elements and beam elements. This model was used to study the global behavior of the heat exchanger and the effects of temperature variations. Shell elements were used to model the channel, shell, flanges, nozzles, support system, shroud, and tubesheet. The tubes were modeled using beam elements.

Once results for the shell models were obtained, the analysis focused on a second model. This submodel used solid, brick elements for the flange and tubesheet, while the bolting was modeled using beam elements. Displacements from the global model were used to induce bending in the submodel that resulted from the bowing of the shell. The submodel permitted the calculation of thru-wall temperature gradients and stress distributions. Along with obtaining greater deflection accuracy in the vicinity of the flange, the submodel also permitted an analysis of the contact stresses on the gaskets of the main body flange.

The third model type involved axisymmetric, continuum elements. Axisymmetric models permit the analysis of stresses that are developed in structures that have loads and geometries that do not vary circumferentially.

The sections that follow provide specific details on each of the three model types and how each contributed to developing an overall understanding about the behavior of the heat exchanger.

Global Model Using Shell Elements

The global analysis used finite element models that incorporated all major components of the heat exchanger. Due to the symmetric behavior of the geometry and loading, a half-symmetry model was used. In addition to the introduction of the symmetry plane, several other simplifications were made to improve modeling efficiency. Details are provided in the sections that follow.

Geometric Symmetry and Boundary Conditions. All of the sources of loading in the heat exchanger are symmetric, including the bolt makeup forces that are axisymmetric. For this reason, a half-symmetry model was used that divides the model into two halves along the plane perpendicular to the Z-axis. Shown in **Figure 1** is a schematic side-view of the global finite element models and includes information relating to support boundary conditions. Invoking the plane of symmetry permits movement in the X and Y directions and restricts rotations about the X and Y axes. In terms of a support system, the support pedestal closest to the channel end was fixed, while the far-end pedestal was permitted to slide in response to pressure end loading and thermal expansion of the exchanger in the X-direction. This is consistent with the actual design as noted in the Brown Fintube drawing package. **Figure 2** provides an inside view of the exchanger with certain sections removed to improve visual clarity.

Tube Bundle. The actual heat exchanger has 1,858 tubes (tube dimensions of 0.75-inch OD by 0.065-inch wall thickness). An attempt to model all of the tubes is not necessary as a representative configuration can be developed that possesses the same cross-sectional area, moment of inertia, and relative stiffness. Thirteen (13) tubes were modeled on the top half of the tubesheet and an additional thirteen (13) tubes were modeled on the bottom half. These twenty-six (26) tubes were connected by U-tubes. The ABAQUS PIPE31 element types were used to permit the application of internal pressure as well as temperature variations horizontally and vertically along the length of the tubes.

One of the more important issues associated with modeling the tube bundle is the level of axial rigidity. Because the tubes were not modeled as a single bundle, each of the 26 tubes could be permitted to displace independently relative to one another. However, in actuality the bundle does operate with a level of rigidity that resembles a relatively homogenous unit. The BFT design utilizes an unbaffled heat exchanger configuration.

Insights provided by Brown Fintube indicated that when the tube bundle was picked up from the center or picked up on either end, no appreciable levels of deflection were observed. To calibrate the finite element model, several levels of tube fixity were considered. Results will be presented in a later section of this report. However, the model that most closely resembled the actual behavior of the bundle had nodes that were restricted from moving relative to one another in the X, Y, and Z directions at equally-spaced intervals. To accomplish this in modeling, the ABAQUS constrain equations (*EQUATION cards) were used to define geometric limitations of select nodes within the model.

The bundle was also restricted from moving through the shell by the use of virtual baffles that simulated the presence of actual baffles using the *EQUATION cards. The bundle was attached to the horizontally-oriented long baffle that was connected to the shroud. The shroud was then connected via *EQUATION cards to the shell at the three locations corresponding to the actual baffle positions.

Application of Operating Loads. Once the geometry of the model was completed, the application of operating conditions was considered. The loading of the heat exchanger involves three distinct load types.

- Make-up of bolting
- Internal pressure (tubeside and shellside)
- Elevated temperatures (variation in top and bottom sections)

The shell element global model treated the main body and channel flanges as integral sections. For modeling purposes this assumption is sufficient as it accurately represents the stiffness contribution of the flanges to the overall model. However, as will be discussed in a later section of this report, the solid sub-model included the effects of bolt make-up and gasket-tubesheet-flange interactions.

A heat transfer model was developed to calculate the nodal temperature distributions within the finite element model. The shell (i.e. four-node quadrilateral) elements incorporated the use of film coefficients, while the tube piping elements had actual temperatures imparted to specific nodes. Brown Fintube provided an extensive heat transfer package that included bulk and skin temperature measurements at specific locations within the exchanger. These data were used as input into the finite element model. The bases for these data were shellside inlet/out temperature of 231/619.6 °F and shellside inlet/out temperature of 697/328.3 °F. **Figure 3a** shows the temperature distribution in the heat exchanger shell, while **Figure 3b** shows the thermal profile for the tube bundle with variations in the X-direction (longitudinal) and Y-direction (vertical).

Internal pressure was applied to the appropriate surfaces with a tubeside pressure of 271.7 psi and a shellside pressure of 343.7 psi. The closed channel end (i.e. blind flange) and shellside end (i.e. elliptical head) ensured that appropriate longitudinal stresses in the shell and channel were generated. The inlet and outlet nozzles were also capped to generate pressure end loads at these locations.

Submodel Using Solid Elements

While the intent of the global model was to determine the overall behavior of the vessel in response to pressure and thermal loads, the intent of the submodel was to determine behavior in the vicinity of the main body flange. Initial concerns with the flange region were raised on the assumption that the bowing of the shell and bundle would impact gasket seating stresses. For this reason, the submodel captured the effects of the vertical temperature gradient as well as including displacements from the global model in relation to the in-plane bowing of the shell and tubesheet.

The sections that follow provide details on the boundary conditions, make-up loading, and application of temperature and pressure associated with the submodel.

Geometric Symmetry and Boundary Conditions. As with the global model, a symmetry plane was assumed perpendicular to the Z-axis. **Figure 4** shows the major elements of the model, while **Figure 5** provides a close-up view showing the flanges, bolting, tubesheet, and gaskets. As noted, the thin row of elements on the outside of the tubesheet and inside surface of the flanges represent the 321 stainless steel cladding. Because of the higher coefficient of thermal expansion, it is important to consider this material in the analysis.

In reviewing **Figure 5**, note the use of shell and beam elements on the outer edge of each flange. This technique permits the

application of loads and/or displacements on a solid model using a single line of action. The displacements from the global model were used to create the in-plane bending conditions. Using the shell elements, the exposed edge was displaced based upon data extracted from the global model.

Contact Surfaces and Bolt Makeup. Unlike the global shell and beam model, the solid submodel involved the use of contact surfaces. In finite element modeling, contact surfaces are used when two components come in contact with one another. The generation of contact surfaces prevents one component from passing through another component when the mating surfaces come in contact. Of equal importance, the finite element analysis permits the calculation of local contact pressure stresses and can assist in monitoring variations that may occur. For example, the relative motion of flanges in the problem at hand involves contact pressure variations in both the radial and circumferential directions. The contact pressures on the gasket can serve as an indicator of leakage behavior.

The main body flange has a total of 60 bolts that have a nominal diameter of 1-1/8 inches. To achieve makeup loads the bolts were cooled which caused a reduction in elongation and induced an effective tension. The final makeup condition resulted in a bolt pre-stress of approximately 58 ksi. During the make-up load step, the flanges were brought in contact with the gaskets. The gaskets were then pressed against the tubesheet surfaces to complete the makeup process.

Application of Operating Loads. Once the make-up load step involving bolt tensioning was completed, operating loads were applied. Internal pressure was applied to the inside surfaces of the model (tubeside pressure of 271.7 psi and a shellside pressure 343.7 psi). A pressure end load was applied to one of the free edges to ensure static equilibrium, while a symmetry place was invoked on the other edge. This process ensured that an axial stress would be generated in the finite element model for both the channel and shell sections.

After the pressure loads were applied, nodal temperatures were used as input to generate thermal stresses. Prior to performing any structural analysis, a heat transfer model was generated to calculate the thru-wall temperature distribution. Based upon discussion with Brown Fintube, it was decided to assume that the flanges were not insulated and open to the outside ambient air. **Figure 5** provides a contour plot showing the temperature distribution around the flange. Note that the minimum temperature of 176 °F is calculated on the outside surface of the flange, which is a result of the non-insulated case.

It is clear that one of the biggest factors impacting flange performance is the temperature of the bolts. It is theoretically possible for the bolts to reach an elevated temperature where they lose their pre-load, although for the current problem this is unlikely as the flange in normal operating conditions is not insulated and on average the bolts are going to have a lower temperature than the gasket.

Assuming there is no significant loss in pre-load of the bolting, as the gasket heats up it will generate an expansive load that will act to increase the local contact pressures. This positively influences the sealing behavior of the flange.

Since the reactor was not intended for cyclic service, a shutdown mode was not considered as part of the analysis.

ANALYSIS RESULTS

Because of the complexity of the analysis effort, it is possible to generate a paper that contains a tremendous amount of result data. However, recognizing that the clear objective of this effort was to address flange performance as it relates to leakage, presentation of results is limited. Results for the following topics are provided.

- Discussion on the bundle response to gravity and thermal/pressure loads
- Deformation behavior of the heat exchanger in response to thermal loads in terms of in-plane and out-of-plane bending
- Discussion on stresses in the flange
- Gasket seating performance (including discussion of PVRC method)

Bundle Response to Gravity and Operating Loads

Early in the modeling effort, Stress Engineering Services and Brown Fintube discussed the options in modeling the tube bundle and the effects that tube fixity have on the overall stiffness. Brown Fintube had field experience indicating that no appreciable deflection resulted when the bundle was picked up at its ends or mid-span.

Initial modeling efforts assumed that the tubes could translate longitudinally relative to one another; however, the calculated deflections with gravity-only loading were large. Consequently, Stress Engineering elected to fix movement of the tubes in the X-direction. **Table 1** provides details on the results associated with several model options. Also included were efforts to address shroud thickness and baffle longitudinal position. The U-bend members are not constrained relative to one another in any of the analyses. For this reason, it is not recommended that the results for these members be considered to exactly represent the true behavior of the actual U-bends.

Deformation Behavior of the Heat Exchanger

Prior to performing the analysis, concerns existed regarding the effects of bowing (i.e. in-plane bending) of the shell and tube bundle. The concern was that if the bundle bowed internally that it would impart a sufficient load onto the shell and cause deformation to a level that would lift it off the supports. While there is no doubt that the bundle and shell both deflect, the analysis showed that the shell bows without any influence from the tube bundle. To prove this point an analysis case was run that involved removing the tube bundle from the model. The shell deflected to the same degree that it had when the bundle was present. The obvious conclusion is that the vertical temperature differential in the shell is sufficient to cause it to deform without any influence from the tube bundle. **Figure 6** shows the deflected shape for the global model assuming normal operating conditions (a magnification factor of 7.0 is imposed on this plot).

Recognizing that the focus in the analyses was on the flange region, post-processing the specific models involved monitoring to determine if any significant changes took place in the vicinity of the flanges. It was noted that minimum changes in the flange stresses resulted when variations such as tube fixity, end supports, and nozzle loads were considered. Most models produced flange stresses that ranged between 50 ksi to 54 ksi, while stresses in the vertical top region of the flange were on the order of 10 ksi to 15 ksi. It became clear that the location of the maximum stress was also positioned closer to the axis of bending, indicating that the in-plane bending itself was not the source of the high stresses.

Post-processing efforts were also taken to address displacement perpendicular to the X-axis (radial for the flange). Analysis of the results showed that the vertical temperature gradient is the primary

source of high stresses in the flange region. This is logical as the high temperature in the top portion of the flange(s) causes an outward dilation, while the cooler bottom prevents the distortion. As a result, ovality in the flange forms and a bending stress due to thermal loads is generated. Once this observation was made, it was clear that the primary focus should not be placed upon the in-plane bending loading.

Gasket Seating Performance

The primary focus of this effort has been to address the sealing performance of the flanges considering make-up, pressure, and thermal loads. Numerous resources exist for evaluating gasket leakage performance. One of the newer approaches is based upon methods developed by the Pressure Vessel Research Council (PVRC). The PVRC method incorporates new gasket parameters that are more accurate for determining the leakage performance of a particular gasket/flange design. **Figure 7A, 7B,** and **7C** provide a printout from MathCad showing the calculations associated with this method. As noted, the 1-1/8-inch diameter bolts satisfy the PVRC gasket leakage design criteria. While these calculations consider pressure loads, they do not address the effects of thermal stresses and displacements.

The three-dimensional solid submodel calculates contact pressure as a function of bolt load and operating condition. Several models were run that address variables such as the following.

- Bolt make-up loading
- Internal pressure loads
- Thermal loads and vertical temperature gradient
- Elevated temperature in bolting to 200 °F and 400 °F

Recognizing the limit of variation of the other parameters, the latter variable (bolting temperature) was the one assumed to be the most important consideration. The need for bolt temperatures to be as less than internal operating temperatures is validated in industry by the fact that flanges are often not insulated.

In order to study contact pressures, Stress Engineering Services ran several finite element models and extracted contact pressures in the vicinity of the gasket(s). The average contact pressure per gasket element was calculated as a function of circumferential position. **Figure 8** shows the average contact pressures for make-up, operating loads with bolts at 200 °F, and operating loads with bolts at 400 °F.

In addition to the plotted date, other data were extracted from the finite element model. The average bolt stresses for the makeup, 200 °F, and 400 °F conditions were 58.3 ksi, 77.8 ksi, and 58.2 ksi, respectively. The average gasket contact stresses for the makeup, 200 °F, and 400 °F conditions were 25.8 ksi, 71.6 ksi, and 63.9 ksi, respectively.

There are several important observations made in viewing the results from **Figure 8** and the data presented in the previous paragraph.

- The introduction of operating pressures and temperatures act to increase the contact stresses in the gasket. This is to be expected as the gasket is made from stainless steel and has a relatively high coefficient of thermal expansion. The fact that the gasket has a higher temperature than the outer region of the flange and bolts also contributes to the increased stress.
- As expected, the increase in bolt temperature acts to decrease the contact pressures in the gasket region. It is theoretically possible that if the bolting temperature reached a sufficiently high level, all pre-load could be lost and the gasket would leak. This is an unlikely scenario considering that the flanges will not be insulated and that the internal operating temperature of the exchanger will always be greater than the external ambient temperatures.
- Even at 200 °F the contact pressures in the gasket do not fall below the original makeup conditions. The minimum contact stress when the bolt temperature is 400 °F is 16,200 psi, which is less than the minimum contact stress at makeup which is 20,100 psi. If the minimum contact stress at 400 °F is multiplied by the gasket seating area of 74.6 in^2, the seating force is approximately 1.5 millions lbs. This value exceeds the PVRC-calculated seating load (see **Figures 7A**, 7**B**, and 7**C**) of 1.06 millions lbs.

Stresses in the Flange Region

Stress Engineering Services performs a significant number of ASME Boiler & Pressure Vessel Code, Section VIII, Division 2 (Code) analyses every year that involve finite element analyses. These efforts involve the calculation of detailed stresses in areas of interest within a vessel for comparison with code allowable stresses. As an example, stress classification involves the following types of stresses.

- General primary membrane stresses
- Local primary membrane stresses
- Primary bending stresses
- Secondary stresses
- Peak stresses

From an analyses standpoint, component stresses in the area of interest are extracted from the finite element model. From the component stresses the principal stresses are computed. For cyclic service considerations, care should be made to integrate the extremes (i.e. minimum and maximum load levels) of the operating cycle(s) in calculating the component stresses. For purposes of comparison with the Code, linearized stresses for each section of interest within the model are obtained. The linearization process permits the calculation of a linearized stress profile through the given section that has the same net bending moment as the actual stress profile. As an outgrowth of this effort, the *Membrane* (Pm) and *Membrane plus Bending* (Pm + Pb) stresses are extracted. Stress intensity (maximum principal stress minus minimum principal stress) is the design stress criteria currently used by the Code. These calculated stress intensities are then compared to the Code-specified stress limits for the respective material at temperature and stress classification.

The high stresses that are generated in the flange are the result of thermal loads that are classified as Secondary Stresses. According to the Code, the stress limit for secondary stresses is $3S_m$. When S_m is governed by yield strength (as it often is at elevated temperature), the $3S_m$ value corresponds to two times yield strength. According to the ***Criteria of the ASME Boiler & Pressure Vessel Code for Design by Analysis in Sections III and VIII***, ***Division 2***, secondary stress is explained as follows.

> *Secondary stress is a stress developed by the self-constraint of a structure. It must satisfy an imposed strain pattern rather than being in equilibrium with an external load. The basic characteristic of a secondary stress is that it is self-limiting. Local yielding and minor distortions can satisfy the discontinuity conditions or thermal expansions which cause the stress to occur.*

Another section of this document provides equally important insights.

> *The primary plus secondary stress limits are intended to prevent excessive plastic deformation leading to incremental collapse, and to validate the application of elastic analysis when performing fatigue evaluation.*

The stress limit for primary membrane plus secondary stress is $3S_m$. This stress level is the maximum value of calculated secondary elastic stress which will shake down to purely elastic action. The level is deemed safe since a small amount of plastic action during overloads is permissible.

For the flange material (SA-182), the design stress intensity values, Sm, for Class 1 and 2 as function of temperature are as follows per Division 2.

- 200 °F Class 2: 23.3 ksi Class 1: 18.5 ksi
- 300 °F Class 2: 23.3 ksi Class 1: 17.5 ksi
- 400 °F Class 2: 22.5 ksi Class 1: 16.9 ksi
- 500 °F Class 2: 21.7 ksi Class 1: 16.3 ksi
- 600 °F Class 2: 20.9 ksi Class 1: 15.7 ksi
- 700 °F Class 2: 20.1 ksi Class 1: 15.1 ksi

The maximum allowable stress for the flange material according to Division 1 is 20 ksi for temperatures up to and including 700 °F. If an analysis is performed on a section of the flange at 600 °F, the limits for primary membrane plus secondary stresses are 62.7 ksi and 47.1 ksi for Class 2 and Class 1, respectively.

Because there is no circumferential variation in stresses in the axisymmetric model, the choice of location for selecting stresses is governed by the behavior in the shell model. The results clearly demonstrate that the largest hoop stresses are generated by bending stresses just above and below the longitudinal baffle. Specifically, the largest nodal stresses occurred at 81.4 degrees and 98.6 degrees relative to the top of the flange. This is 8.6 degrees above and below the horizontal centerline of the heat exchanger on both sides.

The location of interest in the main body flange is the intersection between the flange and mating vessel wall. In most flange analyses, this is the region of greatest concern due to the section change between the flange and vessel wall. Thru-wall stresses were extracted from the finite element for all of the required load cases.

Table 2 provides a detailed listing of the combined stresses. The tabulated values represent combinations of stresses from both the axisymmetric and shell models.

In addition to the tabulated results, displaced mesh and stress intensity contour plots provide useful insights into the behavior of the flange assembly. **Figure 9** shows the stress intensity contour plot for make-up plus pressure load case from the axisymmetric model. Stress intensity is defined as the algebraic difference between the minimum and maximum principal stresses, or two times the maximum shear stress. Note that in this figure stress contours that exceed 30.0 ksi are plotted in red.

The stress contour plot has regions with stresses that exceed 100 ksi. These high stresses are modeling artifacts and do not constitute actual elevated stress values. The high stresses in the model exist because the bolt support elements create locally high stresses when reacting against the outer flange surfaces.

Linearized Stress Results

Once the model runs were completed, stresses were extracted from selected locations in the model. As discussed previously, nodal component stresses were extracted from the global shell model at 81.4 degrees and 98.6 degrees. The axisymmetric model had stresses that were constant with respect to circumferential orientation so location was not important. The region of interest is the junction between the flange and shell wall. As observed in the stress contour plots, this region of the flange assembly has the highest stresses. These results are consistent with patterns observed in previous stress analyses of flanges.

Using the combined component stresses as presented in **Table 2**, linearized stresses were calculated. The linearized stress is the linear distribution of stress that has the same net bending moments as the actual stress distribution in the model. This process permits one to calculate the membrane stress as well as the membrane plus bending stresses (and secondary membrane plus bending stresses) in the inner and outer regions of the wall. These stress values are then compared to the appropriate code stress limits. This methodology is consistent with the ASME Boiler & Pressure Vessel Code, Section VIII, Division 2 *Pressure Vessels – Alternative Rules*. The stress limits are based upon the allowable stresses specified in ASME, Section II, Part D for the SA182-F11 Class 2 flange material and the SA193-B7 bolting material.

There are three stress categories that are of interest. Calculation of the linearized stresses for each of these types involved varying combinations of the component stresses.

- Membrane stress – only considers mechanical loads (gravity, nozzle loads, and internal pressure)
- Membrane plus bending stress – only considers mechanical loads (gravity, nozzle loads, and internal pressure)
- Secondary membrane plus bending – considers all forms of loading (makeup, gravity, nozzle loads, thermal, and internal pressure)

In accordance with the Appendix 4 of Division 2, which distinguishes between primary and secondary loading, the *Membrane* and *Membrane plus Bending* stresses require that the makeup loads be subtracted from the design loads. The primary stresses that are generated in the flanges due to pressure and nozzle loads are separated from the make-up of the bolting. To do this, the results of the make-up case are subtracted from the pressure plus make-up case, component by component, before proceeding.

From the linearized output, one can obtain the maximum membrane and membrane plus bending stresses for the respective section. In a similar manner, the linearized secondary membrane plus bending stresses can be calculated by considering the contribution of makeup and thermal loads.

Table 3 provides a detailed listing of the calculated stresses from the finite element models as well as the appropriate stress limits per the Division 1 and Division 2 criterion.

Stresses in the Bolting

In addition to the stresses in the flange, the stresses in the bolting required calculations. The bolt stresses provided in **Table 4** are extracted from the three-dimensional model. This model was used to determine variations in contact pressure in the gasket region of the flange as a function of circumferential position.

Because initial concerns relating to leakage involved bolt temperature, analyses were conducted to address the effects of bolt temperature. For this reason, results for the following load cases are considered.

- Make-up loading only
- Makeup plus operating loads with bolting at 200 degrees F
- Makeup plus operating loads with bolting at 400 degrees F

Because of the circumferential variation in temperature, the bolt stresses around the flange change as a function of position. For this reason, the maximum and minimum bolt stresses were extracted from the three-dimensional solid model and are included in **Table 4**. As noted in this table, the stress differences between make-up and operation do not exceed the bolting stress limit of 25.0 ksi per the Code.

COMMENTS AND CLOSURE

At the request of Brown Fintube, Stress Engineering Services performed a series of analyses to address issues relating to sealing in a high temperature differential heat exchanger. Efforts involved a combination of shell global models coupled with a three-dimensional solid model incorporating bolt makeup loads, contact surfaces, and gasket seating pressures. Calculations were also performed using the PVRC methods for gasket leakage design criteria.

The global model indicated that while the shell and bundle do deflect in-plane due to thermal gradients, the primary source of stress in the flanges involves the large vertical temperature differential that exists. As the top portion of the flanges try to expand, they are prevented from doing do by the cooler bottom halves of the flanges. The location of the maximum stresses in the flange, in conjunction with the displaced shape, supports this observation.

The solid model permitted the calculation of contact stresses in the gasket. From each of the finite element models, stresses were extracted as functions of circumferential position. With an increased bolt temperature to 200 °F, the gasket contact pressure at any point around the circumference of the flange is never less than the contact pressures at makeup loading. Even with the bolts at 400 °F the seating force considering the minimum gasket contact pressure exceeds the PVRC-calculated design seating force.

Using component stresses from the shell global model and an axisymmetric model, linearized stresses were calculated. From this information membrane, membrane plus bending, and secondary membrane plus bending stresses were determined. These values were compared to the respective temperature-dependant stress limits. None of the calculated stresses in the main body flange exceeded the stress limits. Based upon this observation, the design of the flange assembly meets the design criteria per Division 1 and Division 2 of the ASME Boiler & Pressure Vessel Codes.

REFERENCES

1. API 510, *Pressure Vessel Inspection Code - Maintenance Inspection, Rating, Repair, and Alteration*, Seventh Edition, American Petroleum Institute, Washington, D.C., 1992.

2. API 579, *Recommended Practice for Fitness-For-Service and Continued Operation of Equipment*, Washington, D.C., First Edition, January 2000.

3. *ASME Boiler & Pressure Vessel Code, Section VIII. Division 1*, 2001 edition.

4. *ASME Boiler & Pressure Vessel Code, Section VIII. Division 2 - Alternative Rules*, 2001 edition.

5. ASME HPS-2003, *High Pressure Systems*, Published by the American Society of Mechanical Engineers, New York, Date of Issuance: June 18, 2003.

6. Communication with personnel from Brown Fintube including heat transfer/thermal profile data, July 2003.

Table 1 – Calculated Tube Bundle Deflection

Shroud Thickness	Baffle Configuration	Tube Fixity (X is longitudinal)	Load Case	Outer tube end deflection
1/8-inch	No end baffle	Y and Z	Gravity only	-1.23-inches
			Gravity plus Operating	-3.90-inches
1/16-inch	No end baffle	Y and Z	Gravity only	-1.28-inches
			Gravity plus Operating	-4.24-inches
1/32-inch	No end baffle	Y and Z	Gravity only	-1.35-inches
			Gravity plus Operating	-4.71-inches
1/8-inch	***All present***	***X, Y and Z***	***Gravity only***	***-0.06-inches***
			Gravity plus Operating	***-0.85-inches***
1/8-inch	All present	Y and Z	Gravity only	-0.65-inches
			Gravity plus Operating	-2.41-inches

Note:
Values in ***bold italics*** represent actual conditions of tube bundle based upon BFT static field deflection measurements.

Table 2 – Combined Stresses from Shell and Axisymmetric Models

COMBINED STRESS VALUES (INCLUDING MAKEUP, NOZZLE LOADS, PRESSURE, AND TEMPERATURE)							
Location	**Wall Position**	**Radius**	**S11 (total)**	**S22 (total)**	**S33 (total)**	**S12 (total)**	**S23 (total)**
Top (81.4 deg)	Inside	23	426	-19098	-24616	197	-36
Top (81.4 deg)	Middle	23.375	816	4649	-16599	305	-981
Top (81.4 deg)	Outside	23.75	-1680	37219	-7671	2435	-1925
Bottom (98.6 deg)	Inside	23	426	-9658	49387	197	1419
Bottom (98.6 deg)	Middle	23.375	816	6137	50809	305	993
Bottom (98.6 deg)	Outside	23.75	-1680	31211	53598	2435	568
COMBINED STRESS VALUES (INCLUDING MAKEUP, NOZZLE LOADS, AND PRESSURE)							
Location	**Wall Position**	**Radius**	**S11 (total)**	**S22 (total)**	**S33 (total)**	**S12 (total)**	**S23 (total)**
Top (81.4 deg)	Inside	23	426	-15297	13442	197	675
Top (81.4 deg)	Middle	23.375	816	4040	19856	305	660
Top (81.4 deg)	Outside	23.75	-1680	33465	27445	2435	646
Bottom (98.6 deg)	Inside	23	426	-16440	13497	197	517
Bottom (98.6 deg)	Middle	23.375	816	4032	19920	305	530
Bottom (98.6 deg)	Outside	23.75	-1680	33592	27519	2435	542
COMBINED STRESS VALUES (INCLUDING PRESSURE AND NOZZLE LOADS)							
Location	**Wall Position**	**Radius**	**S11 (total)**	**S22 (total)**	**S33 (total)**	**S12 (total)**	**S23 (total)**
Top (81.4 deg)	Inside	23	-1208	4597	5072	-145	675
Top (81.4 deg)	Middle	23.375	-657	646	4082	-430	660
Top (81.4 deg)	Outside	23.75	99	-2447	3201	-267	646
Bottom (98.6 deg)	Inside	23	-1208	3454	5127	-145	517
Bottom (98.6 deg)	Middle	23.375	-657	638	4146	-430	530
Bottom (98.6 deg)	Outside	23.75	99	-2320	3275	-267	542

Table 3 – Comparison of Linearized Stresses to Allowable Stresses

Location	Membrane Stress, P_m (ksi)	Membrane Stress Limit (ksi)	Membrane + Bending Stress, $P_m + P_b$ (ksi)	Membrane + Bending Stress Limit (ksi)	Secondary Membrane + Bending Stress, $P_m + P_b + Q$ (ksi)	Secondary Membrane + Bending Stress Limit (ksi)
Division 2 Stress Limits						
TOP (81.6° from flange top) ***650°F***	***4.92***	20.5 (kSm)	***6.74***	30.75 (1.5kSm)	***43.19***	61.5 (3.0kSm)
BOTTOM (98.6° from flange top) ***300°F***	***4.94***	23.3 (kSm)	***5.70***	34.95 (1.5kSm)	***61.10***	69.9 (3.0Sm)
Division 1 Stress Limits						
TOP (81.6° from flange top) ***650°F***	***4.92***	20.0 (S)	***6.74***	30.0 (1.5S)	***43.19***	61.6 (2.0Sy)
BOTTOM (98.6° from flange top) ***300°F***	***4.94***	20.0 (S)	***5.70***	30.0 (1.5S)	***61.10***	70.2 (2.0Sy)

Notes:
1. All tabulated stress limits correspond to data for SA182 F11 Class 2 material (Division 1 and 2, respectively).
2. The different allowable stresses used for the top and bottom are due to the temperature differences that exist between these two regions. The temperatures associated with the stress limits are conservatively larger than the actual local temperatures in the flange assembly.
3. Calculated stress values were obtained using finite element methods and linearizing stresses across the respective section of the model.
4. Division 2 stress limits based upon rules specified in Appendix 4 – *Mandatory Design Based Upon Stress Analysis.*
5. Division 1 stress limits based upon rules specified in UG-23. Specifically, per paragraph (e) primary plus secondary stresses are limited to twice yield (2Sy).
6. Earthquake and wind loading not considered, k = 1.0.

Table 4 – Bolt Stresses as Functions of Position and Temperature

Load Case	Bolt Position	Average Bolt Stress (ksi)	Bolt Stress minus Makeup Stress (ksi)
Makeup	N/A	52.1	N/A
Makeup plus operating (bolts at 200 °F)	Top of flange (max)	77.8	25.7
	87° from flange top (min)	58.8	6.7
Makeup plus operating (bolts at 400 °F)	Top of flange (max)	58.3	6.2
	87° from flange top (min)	41.3	(-) 10.8

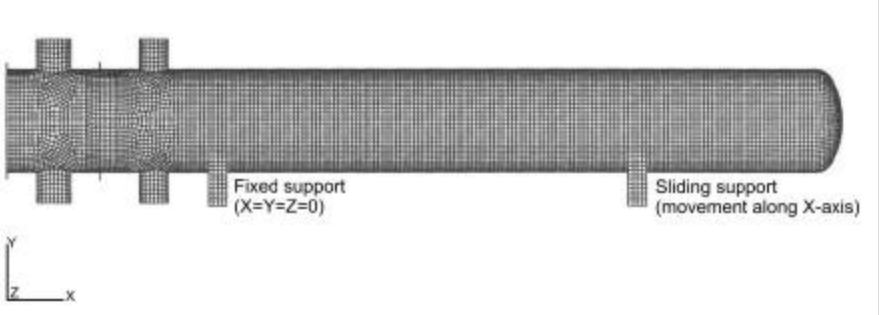

Figure 1 – Schematic side view of the global shell model

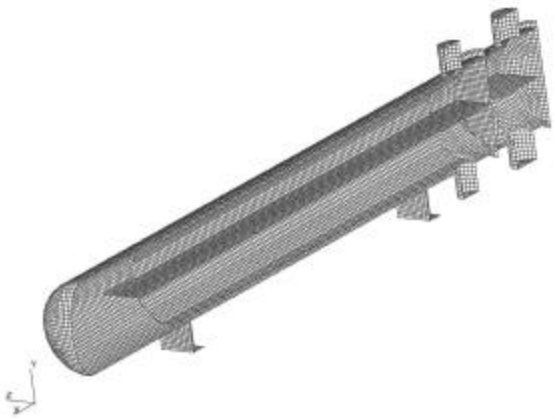

Figure 2 – Inside view of the shell global model with the tubes removed

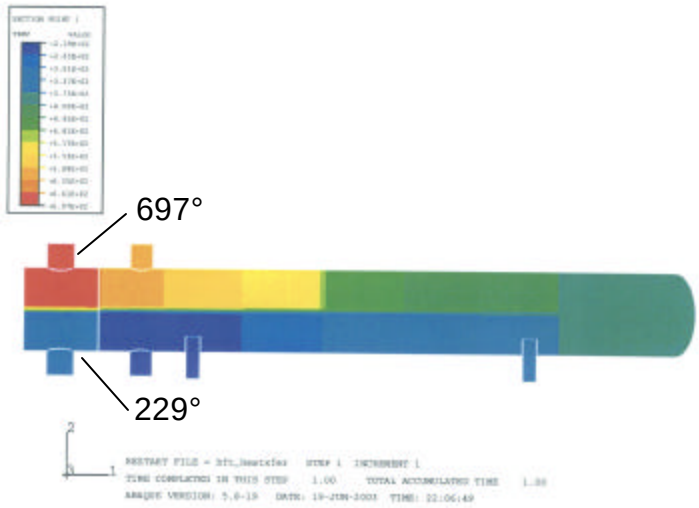

Figure 3a – Temperature distribution in the heat exchanger shell

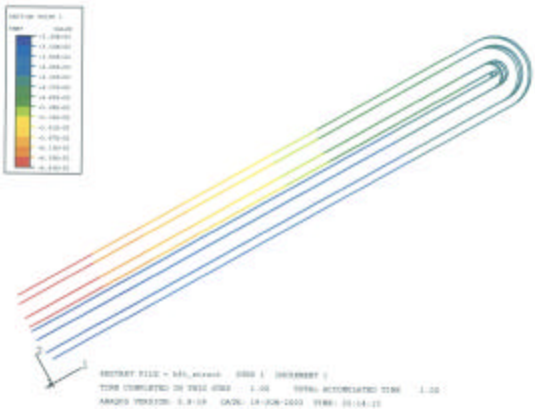

Figure 3b – Temperature distribution in the tubes (variation in X and Y directions)

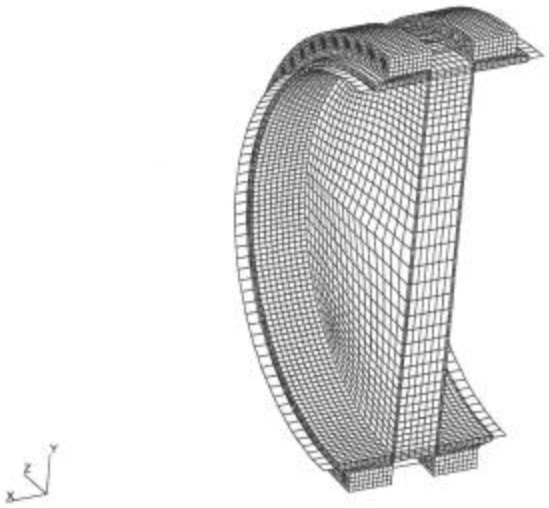

Figure 4 – View of solid submodel along Z-axes cut-plane

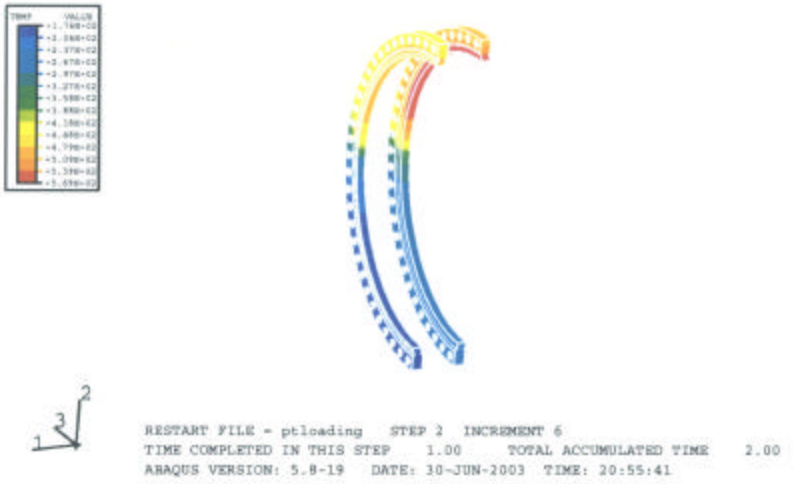

Figure 5 – Temperature distribution in the solid submodel

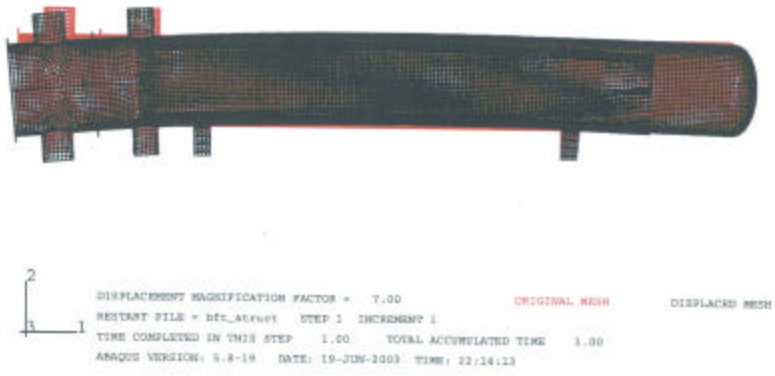

Figure 6 - Deflected shape for the global model with normal operating conditions

PVRC Gasket Leakage Design Method

The following calculations provide detailed results on design of the gasket seating area using the methods developed by the Pressure Vessel Research Council relative to a specified leakage criteria.

The steps below are based upon methods available from Flexitallic's web site, www.flexitallic.com. Brown Fintube provided data for the gasket including Gs, Gb, a, and the tightness class.

To ensure that the results are not overly conservative, the lower tightness class, Tc, and the larger bolt-up efficiency, e, have been selected. For purposes of using MathCAD, unitless values are used.

$P_d := 415$ $P_t := 1.5P_d$ Design and *assumed test* pressures (psi)

$OD_G := 48$ $ID_G := 47$ Gasket outer and inner diameters (inches)

$Sa := 25000$ ***Allowable bolting stress at temperature (psi)***

$D_{bolt\_circle} := 51.25$

$N_{bolts} := 60$

$d_{bolt} := 1.125$

Geometry data on bolting including diameter of bolt circle (inches), number of bolts, and nominal diameter of bolts (inches).

1. Select ***Tightness Class***, Tc, that corresponds to acceptable leakage rate.
   T2 - Standard - mass leakage rate per unit diameter of 0.002 mg/sec/mm-dia
   T3 - Tight - mass leakage rate per unit diameter of 0.00002 mg/sec/mm-dia

2. Select the ***Tightness Constant***, C, that corresponds to the selected Tightness Class.
   C = 1.0 for tightness class T2 (Standard)
   C = 10.0 for tightness class T3 (Tight)

$C := 1.0$ ***T2 tightness class selected***

3. Select the appropriate gasket constants for the selected gasket style and material.

$G_b := 2900$

$a := 0.231$

$G_s := 15$

4. Determine the gasket parameters.

$N := 0.5$ $S_L := 900$ **SL = 900** psi for standard and soft ROTT gasket test procedures
SL = 1,500 psi for the hard gasket test procedures

$b := 0.25$

$G := 47.5$

Figure 7A – MathCad sheet detailing PVRC gasket leakage design calculation

5. Gasket seating area, A_g.

$$A_g := \frac{\pi}{4}\cdot\left(OD_G^{\,2} - ID_G^{\,2}\right) \qquad A_g = 74.6$$

6. Hydraulic area, A_i.

$$A_i := \frac{\pi}{4}\cdot G^2 \qquad A_i = 1772.1$$

7. Minimum tightness parameters, T_{pmin}.

$$T_{pmin} := 0.1243\cdot C\cdot P_d \qquad T_{pmin} = 51.6$$

8. Assembly Tightness, T_{pa}.

$$T_{pa} := 0.1243\cdot C\cdot P_t \qquad T_{pa} = 77.4$$

9. Tightness Parameter Ratio, Tr.

$$T_r := \frac{\log\left(T_{pa}\right)}{\log\left(T_{pmin}\right)} \qquad T_r = 1.103$$

10. Calculate operating stress, Sm1.

$$Sm1 := G_s\cdot\left(\frac{G_b}{G_s}\cdot T_{pa}^{\,a}\right)^{\frac{1}{T_r}} \qquad Sm1 = 4413.9$$

11. Gasket seating stress, Sm2. Use the tightness parameter, e:
e = 0.75 for manual bolt-up
e = 1.0 for hydraulic tensioners and ultrasonic

$$e := 1.0$$

$$Sm2 := G_b\cdot\frac{T_{pa}^{\,a}}{1.5\cdot e} - P_d\cdot\left(\frac{A_i}{A_g}\right) \qquad Sm2 = -4577$$

12. Design factors - Mo and Smo..

$$Mo := \max\left(2, \frac{Sm1}{P_d}, \frac{Sm2}{P_d}\right) \quad Mo = 10.6 \qquad Smo := \max\left(Sm1, Sm2, 2\cdot P_t, S_L\right) \quad Smo = 4413.9$$

13. Calculate ***Design Bolt Load***, Wmo (lbs.).

$$Wmo := A_g\cdot Smo + A_i\cdot P_d \qquad Wmo = 1064733$$

Figure 7B – MathCad sheet detailing PVRC gasket leakage design calculation

Calculate required area and diameter per bolt.

$$A_{bolt} := \frac{Wmo}{N_{bolts} \cdot Sa} \qquad A_{bolt} = 0.71$$

The selected bolts must have a minimum area and/or diameter equal to or greater than the calculated values.

$$d_{bolt} := \sqrt{\frac{4}{\pi} \cdot A_{bolt}} \qquad d_{bolt} = 0.951$$

According to the *Machinery's Handbook*, the following areas and diameters are available for 8-series (UN and UNR designations) bolting.

1.125-inch diameter	Minor diameter = 0.9716-inch	Area Minor Diameter = 0.728 in^2
1.1875-inch diameter	Minor diameter = 1.0341-inch	Area Minor Diameter = 0.825 in^2
1.25-inch diameter	Minor diameter = 1.0966-inch	Area Minor Diameter = 0.929 in^2

NOTE: The 1.125-inch diameter bolts satisfy the PVRC gasket leakage design criteria using the data provided for the Brown Fintube Heat Exchanger assuming B7 bolts (as opposed to B7M with an allowable stress of 20 ksi).

Figure 7C – MathCad sheet detailing PVRC gasket leakage design calculation

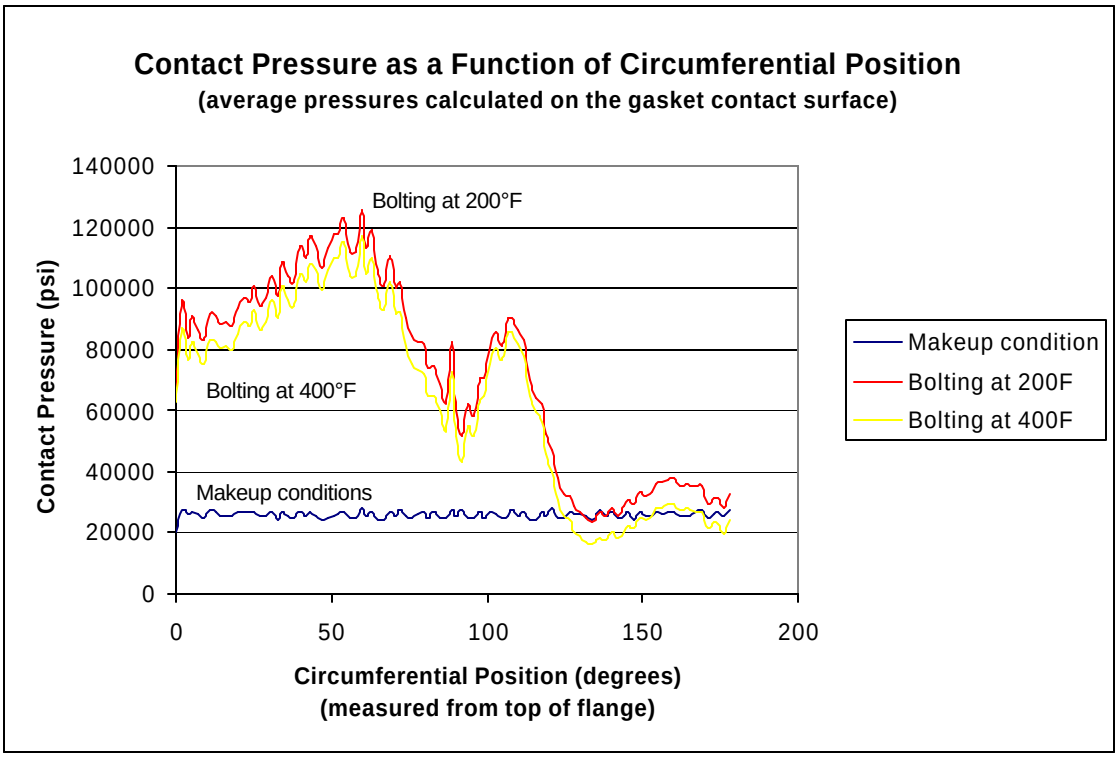

Figure 8 – Contact stresses on gasket face for selected load states

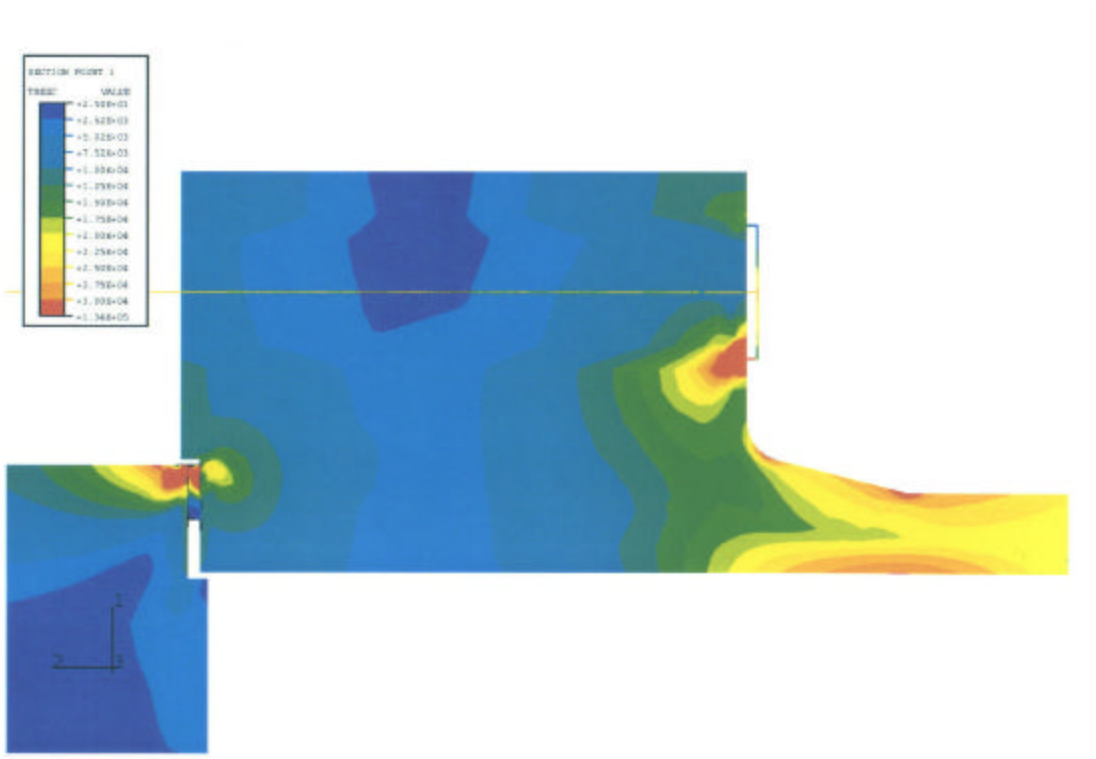

Figure 9 – Stress Intensity Contour Plots for Makeup plus Pressure Load Case
*(contour regions plotted in **red** exceed 30 ksi)*